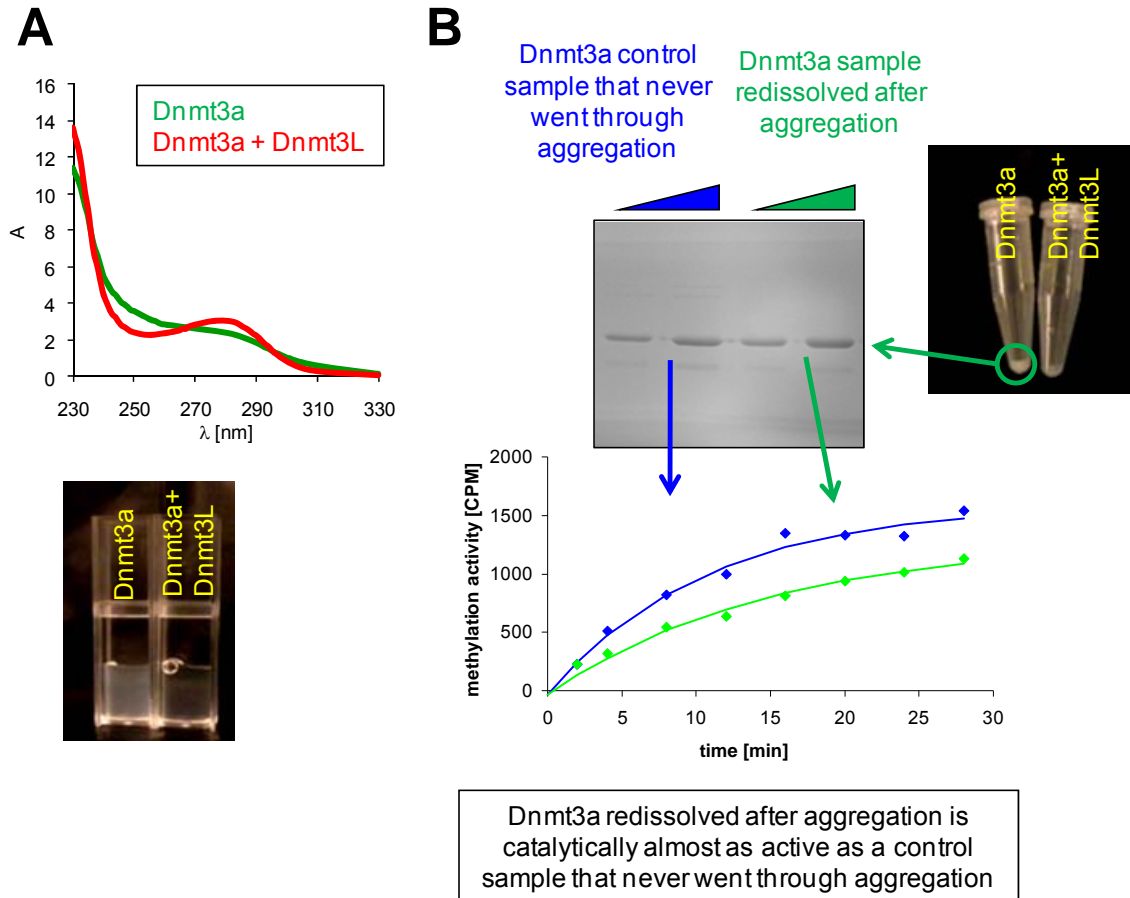


**OLIGOMERIZATION AND BINDING OF THE DNMT3A DNA  
METHYLTRANSFERASE TO PARALLEL DNA MOLECULES,  
HETEROCHROMATIC LOCALIZATION AND ROLE OF  
DNMT3L\***

Renata Z. Jurkowska, Arumugam Rajavelu, Nils Anspach, Claus Urbanke, Gytis Jankevicius, Sergey Ragozin, Wolfgang Nellen & Albert Jeltsch

**Contents:**

Supplemental Figures S1-S7



### Supplemental Figure 1

A) Aggregation of Dnmt3a-C (40  $\mu$ M) occurs during reduction of salt concentration from 500 mM KCl to 200 mM KCl by 2 hours of dialysis. Presence of equal amounts of Dnmt3L-C prevented the aggregation. Aggregation is visible in the UV spectra of the samples and in the turbulent appearance of the Dnmt3a-C solution.

B) Active Dnmt3a can be recovered from aggregated material. Aggregated Dnmt3a-C was dissolved in Dnmt3a-C storage buffer (20 mM Hepes pH 7.2, 200 mM KCl, 1 mM EDTA, 0.2 mM DTT and 10% glycerol). Afterwards the amount of redissolved enzyme was determined and its catalytic activity assessed using an enzyme preparation that never went through precipitation as reference. Kinetics were carried out using 2  $\mu$ M of enzyme, 1  $\mu$ M 30mer oligonucleotide substrate in methylation buffer (20 mM Hepes pH 7.2, 50 mM KCl, 1 mM EDTA, 0.025 mg/ml BSA) at 37°C as described (40). Note that highly active Dnmt3a could be recovered from the precipitated material (with about 80% of specific activity) although the procedure did not include any refolding step.

**A**

→ start of C-terminal domain

```

3a_mouse: CVDLLVGPAAQAAIKEDPWNCYMCGHKGTYGLLRRRDKWPSRLQMFANNHD...QEFDPKVPYPPVPAEKRRKPIRVLSLFDGI : 639
3a_human: CVDLLVGPAAQAAIKEDPWNCYMCGHKGTYGLLRRRDKWPSRLQMFANNHD...QEFDPKVPYPPVPAEKRRKPIRVLSLFDGI : 643
3b_mouse: CLEVLVCAATAEDAKLOEPWSCYMLPQRCHGVLRRRDKWNMRLQDFFTDDELEEFEPKLYPAIPAAKRRPIRVLSLFDGI : 590
3b_human: CLEVLVCAATAEAALQEPWSCYMLPQRCHGVLRRRDKWNMRLQDFFTDDELEEFEPKLYPAIPAAKRRPIRVLSLFDGI : 584
3L_human: CVDLLVGPPTSCKVHAMSNNVCMCLCLPSSRSGLLQRRKWRSQLKAFYDRSE...NPDEMFTVPVWRQPPVRLSLFDGI : 199
3L_mouse: CVDLLVGPPTSERINAMACWVCLCLPFSRSGLLQRRKWRSQLKAFHDCEGA...GPMETIKTVSAWKRPVRLSLFRNI : 233

3a_mouse: ATGLLVKLDLGIQVDRIYASEVCEDSITVGMVRHQGKIMYVGDVRSVTQKHIEQWGPFDLVIGGSPCNDSLIVNPAKGLYEG : 722
3a_human: ATGLLVKLDLGIQVDRIYASEVCEDSITVGMVRHQGKIMYVGDVRSVTQKHIEQWGPFDLVIGGSPCNDSLIVNPAKGLYEG : 726
3b_mouse: ATGYLVKELGKIKVKEYVASEVCEESIAVGTVKHEGQIKYVNDVRNITKKNIEEWGPFDLVIGGSPCNDSLIVNPAKGLYEG : 673
3b_human: ATGYLVKELGKIKVKEYVASEVCEESIAVGTVKHEGQIKYVNDVRNITKKNIEEWGPFDLVIGGSPCNDSLIVNPAKGLYEG : 667
3L_human: KK...ELTSLGFLES.....GSDFG...CLKHVVVDVDTVIRKQDVEEWGPFDLVYG.....ATFPLGHTCDRP : 255
3L_mouse: DK...VLKSLGFLES.....GSGSGCGTILKYVEDVTNVVRRDVEKRWGPFDLVYG.....STCPLGSSCDRC : 291

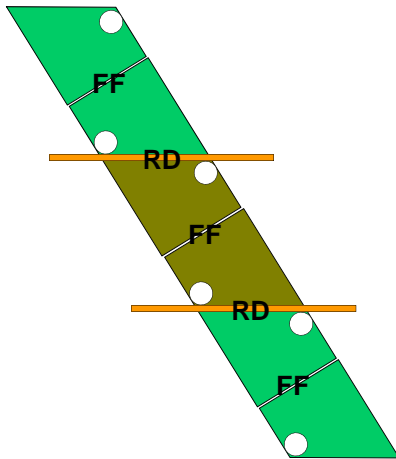
3a_mouse: TGRLEFEFYRLLDHARPKEGDDRPFFWLFENVVAMGVSDKRDISRFLSNPVMIDAKEVSAHRARYFWGNLPGMNRPLASTV : 805
3a_human: TGRLEFEFYRLLDHARPKEGDDRPFFWLFENVVAMGVSDKRDISRFLSNPVMIDAKEVSAHRARYFWGNLPGMNRPLASTV : 809
3b_mouse: TGRLEFEFYHLLNYPKPEGDNRPFFWLFENVVAMKVNDKRDISRFLSNPVMIDAKEVSAHRARYFWGNLPGMNRPLASTV : 756
3b_human: TGRLEFEFYHLLNYPKPEGDDRPFFWLFENVVAMKVNDKRDISRFLSNPVMIDAKEVSAHRARYFWGNLPGMNRPLASTV : 750
3L_human: PSWYLFQFHRLLQYARPKGSRPFFWLFENVVAMKEDLVASRFLSNPVMIDAKEVSAHRARYFWGNLPGMNRPLASTV : 338
3L_mouse: PGWMLFQFHRLLQYALPROESRPFWLFENVVAMKEDLVASRFLSNPVMIDAKEVSAHRARYFWGNLPGMNRPLASTV : 373

3a_mouse: NDKLELQECLEHGRIAKFSKVRTITTRSNSIKQGKDQHFVFMNEKEDILWCTEMERVFGFPVHYTDVSNMSRLAKQRLLSRS : 888
3a_human: NDKLELQECLEHGRIAKFSKVRTITTRSNSIKQGKDQHFVFMNEKEDILWCTEMERVFGFPVHYTDVSNMSRLAKQRLLSRS : 892
3b_mouse: NDKLELQDCLEFSRTAKLKKVQTIITTKSNSIRQGNQLFPVVMNGKEDDLWCTELERIFGFPAHYTDVSNMGRGARQKLLRS : 839
3b_human: NDKLELQDCLEYNRIAKLKKVQTIITTKSNSIKQGNQLFPVVMNGKEDDLWCTELERIFGFPAHYTDVSNMGRGARQKLLRS : 833
3L_human: VSEELSLAQNQSSKLAKWPTKLVKNCPLPLREYFKYFSTELTSSL. : 387
3L_mouse: TPKEEYLQAGVRSRSLDAPKVDLLVKNCLPLPLREYFKYFSONSLPL.. : 421

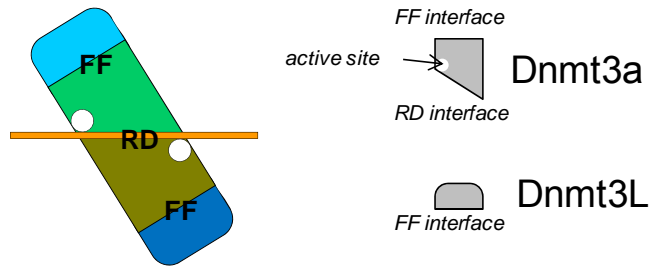
3a_mouse: WSPVIRHLFAPLKEYFACV : 908
3a_human: WSPVIRHLFAPLKEYFACV : 912
3b_mouse: WSPVIRHLFAPLKDYFACE : 859
3b_human: WSPVIRHLFAPLKDYFACE : 853

```

**B**



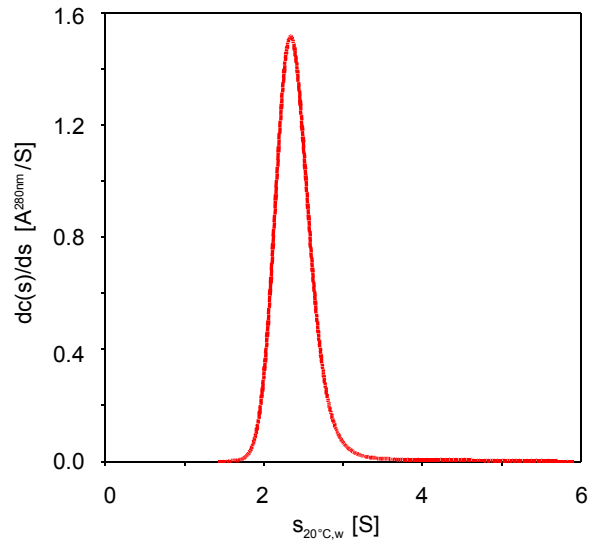
**C**



## **Supplemental Figure 2**

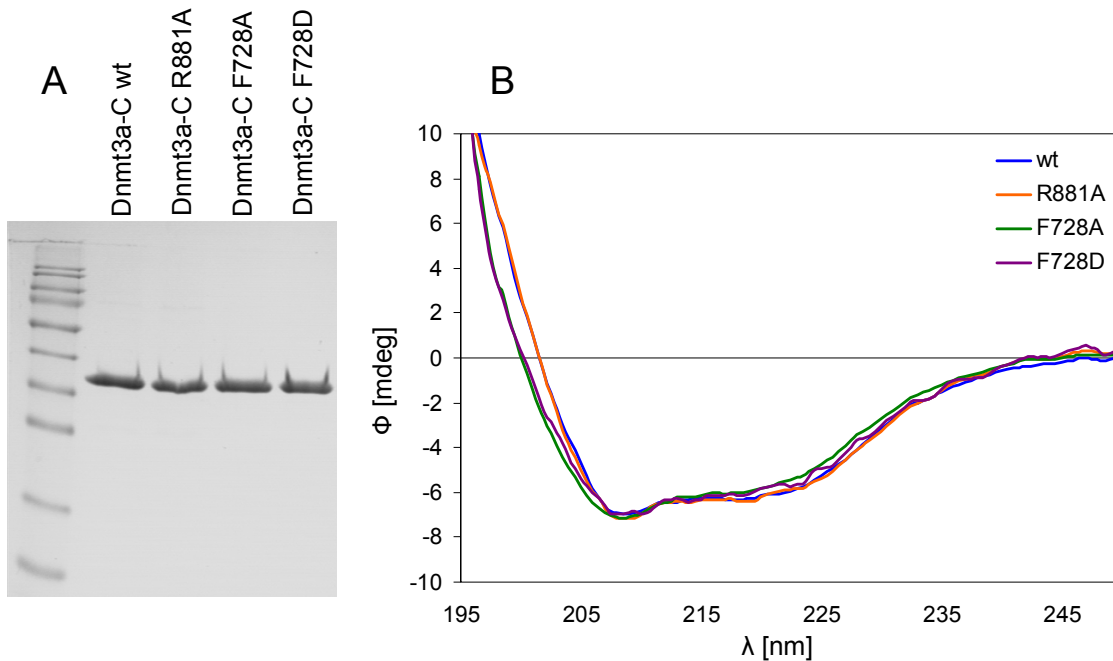
A) Sequence alignment of the C-terminal parts of the human and mouse Dnmt3 enzymes showing the similarity of the FF and RD interfaces. Residues from the RD and FF interfaces are labeled in orange and red, respectively, the main residues involved in the interaction at both interfaces (F728, F768 at the FF interface and R881 and D872 at the RD interface) are shaded in blue.

B and C) Schematic pictures of the multimeric structure of Dnmt3a (B) and the Dnmt3a/3L heterotetramer (C). In either case oligomers are formed by RD interface interaction of dimers formed via the FF interface. Dnmt3a is colored light green and dark olive green, Dnmt3L cyan and blue and bound DNA is shown as orange line. Dnmt3a oligomers can bind to more than one DNA molecule oriented in parallel.



### Supplemental Figure 3

Monomeric state of Dnmt3L-C. Analytical centrifugation analysis of 9  $\mu$ M Dnmt3L-C at 8 $^{\circ}$ C and 45 krpm in 10 mM HEPES pH 7.2, 0.15 M KCl, 1.34 M glycerol (10%), 1 mM EDTA, and 0.2 mM DTT. The figure shows the differential sedimentation coefficient distribution. Dnmt3L-C sedimented with a sedimentation constant of 2.35 corresponding to a monomeric state (frictional ratio 1.35).

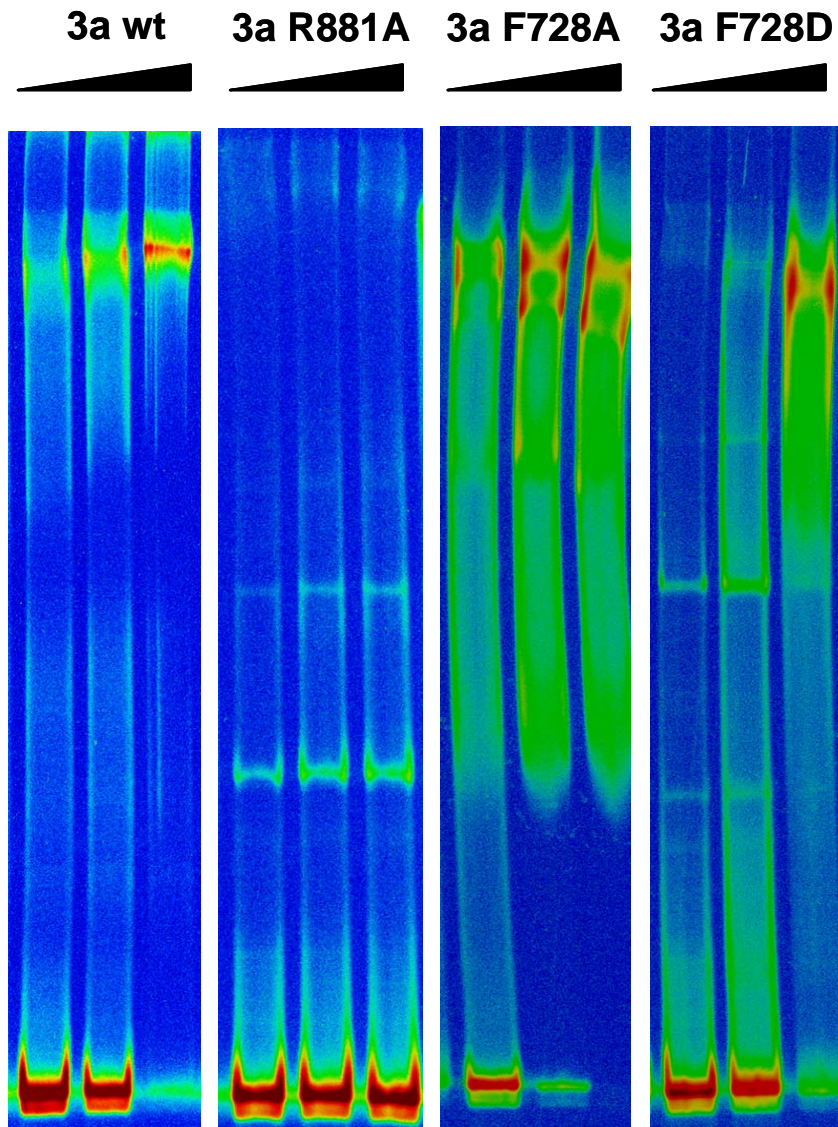


#### Supplemental Figure 4

Purification and folding of Dnmt3a-C wt and its interface variants.

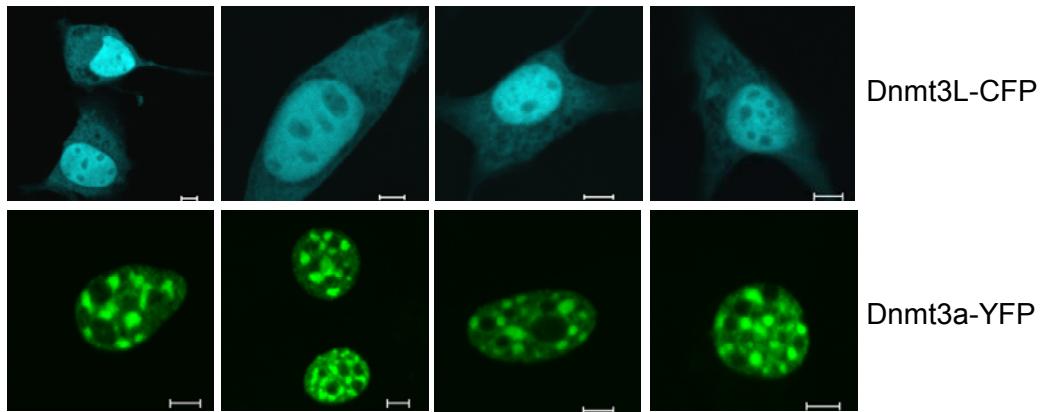
A) SDS-gel stained with colloidal Coomassie showing similar quality and amount of the Dnmt3a-C wt and its interface variants R881A, F728A and F728D. The purity of the proteins was estimated to be 98%.

B) Far UV circular dichroism spectra of the Dnmt3a-C wt and its interface variants. The figure shows superposition of the experimental curves obtained for the wt and mutant proteins. It demonstrates that the folding of the R881A mutant is identical to that of the wt protein. The F728A and F728D mutants show a change in the ascending limb of the spectrum around 200 nm, suggesting some deviation from the wt folding but the CD spectrum clearly indicates that both variants are folded.



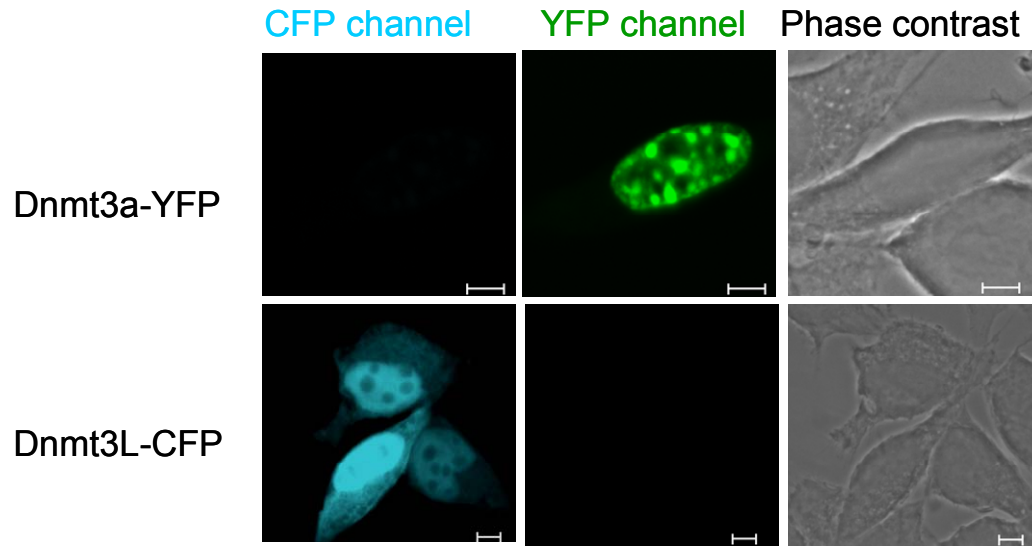
### Supplemental Figure 5

DNA binding and filament formation by Dnmt3a-C wt and its interface mutants. DNA binding of wt Dnmt3a-C, and its R881A, F728A and F728D variants was determined by electromobility shift assays using fluorescently labeled 146-bp long DNA (30 nM) and increasing amounts of proteins (1–10  $\mu$ M) in reaction buffer (20 nM HEPES pH 7.5, 1 mM EDTA, 100 mM KCl, 0.2 mM sinefungin, 0.5 mg/ml BSA) basically as described (38, 40). Sinefungin is an analog of AdoMet that does not allow DNA methylation but supports DNA binding of Dnmt3a-C. The gel was then scanned with a phosphoimager system (Fuji).



### Supplemental Figure 6

Localization of the ectopically expressed, YFP-tagged Dnmt3a and CFP-tagged Dnmt3L in NIH3T3 cells. Dnmt3a is localized uniquely to the nucleus and concentrates in the heterochromatic spots, while Dnmt3L in the absence of Dnmt3a is present both in the nucleus and in the cytoplasm. The scale bars represent 5  $\mu\text{m}$ .



**Supplemental Figure 7**

**Localization of Dnmt3a in NIH3T3 cells in the presence and absence of Dnmt3L.** Control experiment showing that under experimental settings used here there is no cross-talk between the CFP and the YFP channels. The scale bars represent 5  $\mu\text{m}$ .